JACS
JOURNAL OF THE AMERICAN CHEMICAL SOCIETY
Article
pubs.acs.org/JACS

A Synthetic Receptor for Asymmetric Dimethyl Arginine

Lindsey I. James,[¶,‡] Joshua E. Beaver,[¶] Natalie W. Rice, and Marcey L. Waters*

Department of Chemistry, CB 3290, University of North Carolina at Chapel Hill, Chapel Hill, North Carolina 27599, United States

Supporting Information

ABSTRACT: Dynamic combinatorial chemistry was utilized to identify a novel small molecule receptor, **A_2D**, for asymmetric dimethyl arginine ($aRMe_2$), which is a post-translational modification (PTM) in proteins. It is known to play a role in a number of diseases, including spinal muscular atrophy, leukemia, lymphoma, and breast cancer. The receptor exhibits 2.5−7.5-fold selectivity over the isomeric symmetric dimethyl arginine, depending on the surrounding sequence, with binding affinities in the low micromolar range. The affinity and selectivity of **A_2D** for the different methylated states of Arg parallels that of proteins that bind to these PTMs. Characterization of the receptor−PTM complex indicates that cation−π interactions provide the main driving force for binding, loosely mimicking the binding mode found in the recognition of dimethyl arginine by native protein receptors.

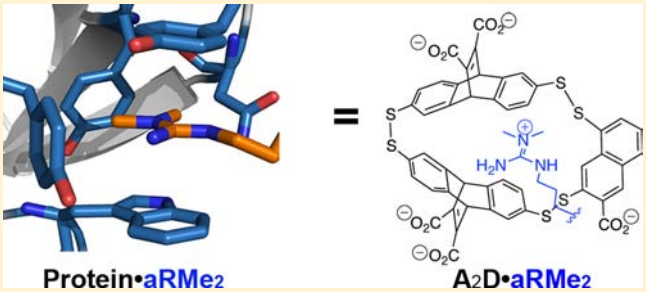

INTRODUCTION

Methylation of arginine (Arg) is a common post-translational modification (PTM) found in both cytoplasmic and nuclear proteins that plays a critical role in many cellular functions, including transcriptional regulation, signal transduction, protein translocation, mRNA splicing, and DNA repair.[1] Protein Arg methyltransferases (PRMTs) methylate Arg (Figure 1), resulting in either monomethyl Arg (RMe), asymmetric dimethylarginine ($aRMe_2$), or symmetric dimethylarginine ($sRMe_2$) depending on the enzyme's specific function.[1] Dysregulation of Arg methylation has been linked to a number of different diseases, including spinal muscular atrophy, leukemia, lymphoma, and breast cancer.[1] Arg methylation has been shown in some cases to inhibit protein−protein interactions, while in other cases it induces protein−protein interactions via specific recognition of the methyl Arg by a 'reader' protein, in turn controlling various downstream biological functions. To date, crystal or NMR structures have been obtained of four tudor domains bound to $sRMe_2$ or $aRMe_2$.[2] In each case, RMe_2 is bound in an aromatic cage of the tudor domain via a combination of CH−π interactions with the $CH_3(\delta+)$ groups, cation−π and π−π stacking of the guanidinium group with two aromatic rings, NH−π interactions, and hydrogen bonds (Figure 2),[2] with binding affinities ranging from 5 μM to >200 μM.[2,3]

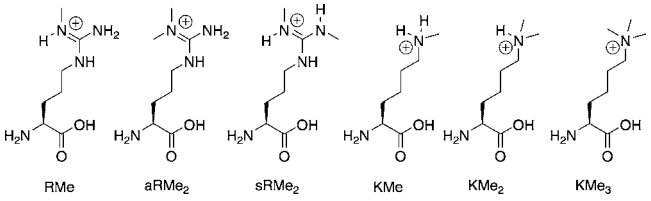

Figure 1. Methylation states of Arg and Lys that are found in proteins.

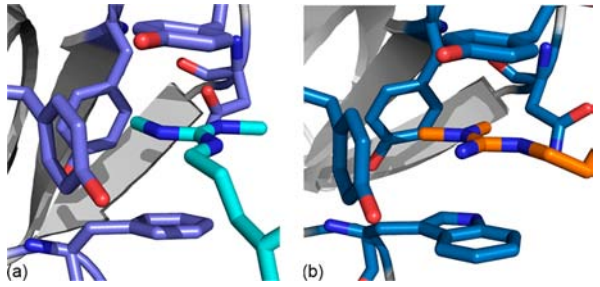

Figure 2. (a) Crystal structure of the SND1 extended Tudor domain bound to $sRMe_2$ (cyan) of PIWIL1 (pdb: 3OMG). (b) NMR structure of the SMN Tudor domain bound to $aRMe_2$ (orange) (pdb: 4A4G).

With the goals of gaining a better understanding of methylarginine recognition and developing new methods for sensing these PTMs, we set out to develop small molecule synthetic receptors for methylated Arg. Previously we reported using dynamic combinatorial chemistry (DCC)[4] to develop a synthetic receptor, **A_2B** (both *rac-* and *meso-*), for another methylated amino acid, trimethyl Lys (KMe_3) (Figure 3). **A_2B** displays affinity and selectivity that is comparable to a native KMe_3 protein receptor.[5] Herein we demonstrate that small structural changes to one of the building blocks that make up **A_2B** result in a new molecule, **A_2D** (Figure 3), that binds $aRMe_2$ with low micromolar affinity and selectively recognizes $aRMe_2$ over $sRMe_2$ and RMe.

Received: August 14, 2012
Published: April 5, 2013

   dx.doi.org/10.1021/ja307907p | J. Am. Chem. Soc. 2013, 135, 6450−6455

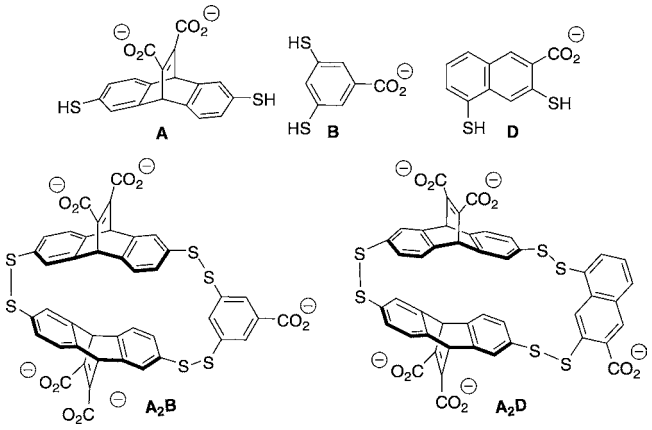

Figure 3. (a) Structure of monomers investigated in DCLs with methylated Lys and Arg guests. Monomer **C** (not shown) was reported previously.[5] (b) Structure of $\mathbf{A_2B}$ (only the *rac*-stereoisomer is shown) that binds KMe_3[5] and $\mathbf{A_2D}$ that binds $aRMe_2$ and KMe_3.

RESULTS

System Design. DCC was used to screen for novel receptors for the different methylation states of Lys and Arg. DCC is an attractive alternative to the rational design of synthetic receptors in that it allows molecular recognition to guide the synthesis of complex host systems from simple building blocks.[4] These building blocks react reversibly to produce an equilibrium mixture of potential receptors. In the presence of a molecular target, favorable host−guest binding interactions drive the synthesis and amplification of favorable receptors at the expense of other species. DCC also allows for parallel screening of the same library of building blocks against all Lys and Arg methylation states, providing a rapid approach to screen for selective recognition of the different PTMs. Disulfide exchange was chosen as the reversible reaction to link the monomeric building blocks because it occurs in aqueous solution at close to neutral pH and is stable toward most biological functional groups.[6] In addition, exchange can be quenched under acidic conditions, allowing for analysis of the library under static conditions.

The previously reported receptor, $\mathbf{A_2B}$, forms an aromatic binding pocket with preference for KMe_3 over the lower methylation states of Lys and all of the methylation states of Arg.[5] Binding occurs via cation−π interactions between the tetraalkyl ammonium group of KMe_3 and the aromatic pocket. The preference for KMe_3 arises from a number of factors including a better fit in the binding pocket and lower desolvation cost than the lower methylation states of Lys as well as favorable CH(δ+)−π interactions.[7] We sought to explore structure−function relationships in $\mathbf{A_2B}$ by replacing monomer **B** with a larger naphthalene-based dithiol, monomer **D**, in a dynamic combinatorial library (DCL) with monomer **A** and evaluating the impact on recognition of methylated Lys and Arg. We hypothesized that incorporation of monomer **D** would provide larger macrocycles which may interact with PTMs that are sterically occluded by $\mathbf{A_2B}$, such as $aRMe_2$ and $sRMe_2$. Additionally, the naphthyl ring of **D** was expected to provide better stacking interactions with the planar Arg side chain than the phenyl ring in **B**. Lastly, similar to $\mathbf{A_2B}$, an aromatic pocket was expected to minimize binding to lower methylation states of Lys and Arg due to unfavorable desolvation costs.[8]

Dynamic Combinatorial Chemistry. Eight separate DCLs biased toward the formation of $\mathbf{A_2D}$ were prepared in which building blocks **A** and **D** were mixed in a 2:1 ratio, respectively, and each was combined with a dipeptide guest, Ac-KMe_x-G-NH_2 (x = 0−3) or Ac-RMe_y-G-NH_2 (y = 0−2), or no guest in the case of the untemplated library. This simple sequence was chosen to minimize interactions with neighboring amino acids, with the hope of amplifying species that bind primarily to the modified side chain. The composition of each library was monitored by LC-MS, and after reaching equilibrium, the receptors that were amplified in the presence of each guest as compared to the untemplated library were identified. Unmethylated Lys and Arg peptides were used to evaluate receptor selectivity for methylated residues over unmodified residues.

Upon templation with $aRMe_2$, $\mathbf{A_2D}$ is strongly amplified, while the amplification by $sRMe_2$ is quite weak in comparison (Figure 4). There are two sets of possible $\mathbf{A_2D}$ diastereomers, however the amplification of only a single $\mathbf{A_2D}$ diastereomer in the presence of methylated PTMs was observed. It should be noted that only one $\mathbf{A_2D}$ isomer exists in high enough concentration to be detected in the untemplated library, indicating significant differences in thermodynamic stabilities between the isomers of $\mathbf{A_2D}$. The amplification of $\mathbf{A_2D}$ in the

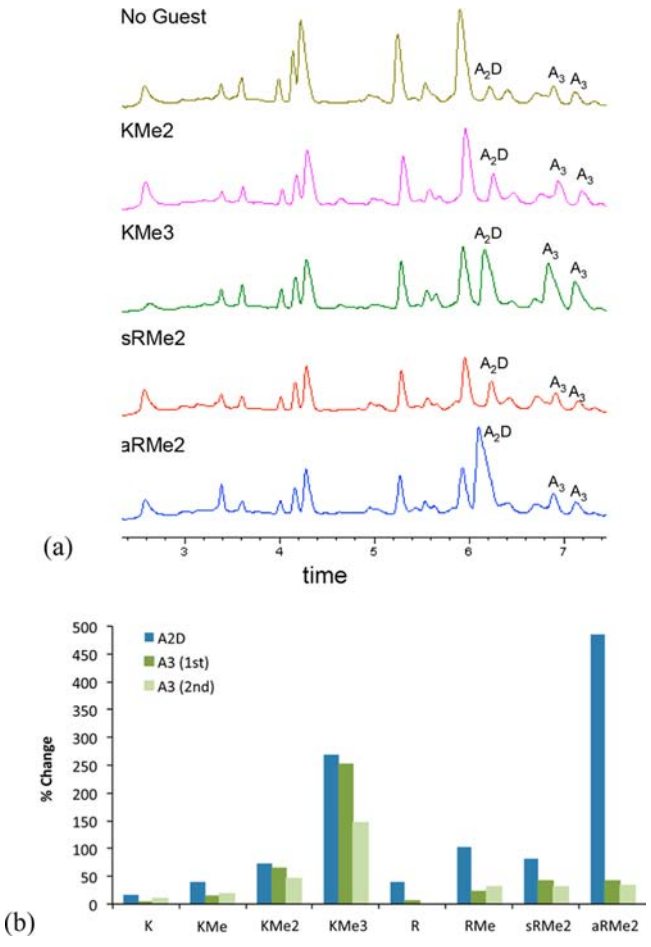

Figure 4. (a) The analytical HPLC traces at 254 nm of DCLs consisting of monomers **A** (5 mM), **D** (2.5 mM), and 7.5 mM guest. The y-axis is absorbance in arbitrary units and all traces are on the same scale. (b) Percent amplification of $\mathbf{A_2D}$ biased libraries templated with Lys and Arg dipeptide guests relative to the untemplated library. The extent of amplification of $\mathbf{A_2D}$ (blue) and both $\mathbf{A_3}$ isomers (green) is shown.

dx.doi.org/10.1021/ja307907p | J. Am. Chem. Soc. 2013, 135, 6450−6455

biased library is also observed with KMe_3, but to a lesser extent than with $aRMe_2$ (Figure 4). Futhermore, templation with KMe_3 also results in a similar degree of amplification of two $\mathbf{A}_3$ isomers.[9]

Structural Characterization. $\mathbf{A}_2\mathbf{D}$ was synthesized on a preparative scale via DCC and purified by RP-HPLC as described in the Experimental Procedures section. NMR studies, including 1D ^{1}H spectra, NOESY, TOSCY, and COSY experiments, were undertaken to characterize the structure of the $\mathbf{A}_2\mathbf{D}$ receptor in both the absence and presence of guest.[10] In characterizing the receptor alone, most notable were the chemical shifts of protons 2 and 3 of the naphthyl ring (Figure 5a), which were shifted to ~3.1 and 2.9 ppm,

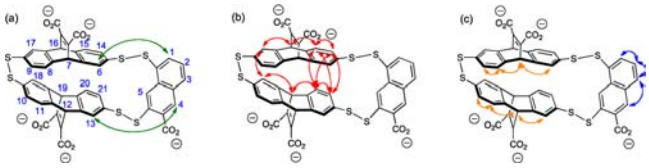

Figure 5. $\mathbf{A}_2\mathbf{D}$ NOESY cross peaks: (a) NOEs between **A** and **D** subunits; (b) NOEs between **A** subunits; and (c) NOEs within subunits.

respectively (see Supporting Information). This is almost 5 ppm further upfield from where these proton signals appear in the spectra of monomer **D**. Based on observed NOEs (Figure 5a) and the significant upfield shift of these naphthalene protons, it is proposed that this portion of the naphthalene ring is directed toward the inside of the receptor cavity, sandwiched between both **A** subunits and packed into the aromatic pocket. Furthermore, the observed $\mathbf{A}_2\mathbf{D}$ isomer is predicted to be the *RR,SS*/*SS,RR* pair of enantiomers due to the presence of NOE cross peaks between four monomer **A** aromatic doublets (protons 14, 15, 20, and 21 in Figure 5), suggesting that they are all in close proximity on one edge of the macrocycle (Figure 5b). While the **A** subunits appear to be in close proximity on one edge of the molecule, no NOEs were observed between protons on the other edge (protons 6−13), suggesting that they are further apart from each other, creating a binding cleft.

NMR was also used to investigate the recognition of $aRMe_2$ and $sRMe_2$ by $\mathbf{A}_2\mathbf{D}$ by evaluating changes in the ^{1}H spectra of the dipeptides, Ac-$aRMe_2$-G-NH_2 and Ac-$sRMe_2$-G-NH_2, upon binding (Table 1). Experiments were performed with 600 μM peptide and a 3−4-fold excess of $\mathbf{A}_2\mathbf{D}$ so that the peptide is in the fully bound state. The peaks for $\mathbf{A}_2\mathbf{D}$ broaden significantly upon mixing, indicating that the rate of exchange is on the NMR time scale. Interestingly, the side chain of both $aRMe_2$ and $sRMe_2$ is also broadened, suggesting that binding can occur in more than one conformation (see Supporting Information for spectra). In the case of $aRMe_2$, more significant upfield shifting is observed for protons closer to the guanidinium group, with the methyl protons shifted to the greatest extent, indicating that they are packed against the face of an aromatic ring. In contrast, upfield shifting is observed to some degree at every position in the $sRMe_2$ peptide, including the Gly protons. While a greater degree of upfield shifting is observed at the α and β positions of $sRMe_2$ than $aRMe_2$, less upfield shifting is observed at the methyl groups. These data suggests that $aRMe_2$ binding stems primarily from interaction with the guanidinium methyl groups, whereas $sRMe_2$ interacts with the receptor at multiple positions along the side chain but with less interaction of the methyl groups. The broadening of the $sRMe_2$ proton signals bound to $\mathbf{A}_2\mathbf{D}$ suggests that it interconverts between inserting one methyl group or the other into the receptor binding pocket, unlike $aRMe_2$, for which the methyl groups give a sharp peak.

Table 1. Change in Chemical Shifts of Ac-$aRMe_2$-G-NH_2 and Ac-$sRMe_2$-G-NH_2 in the Presence of an Excess of $\mathbf{A}_2\mathbf{D}$ Relative to the Unbound State[a]

position	$\Delta\delta$ $aRMe_2$	$\Delta\delta$ $sRMe_2$
Ac	0.03	−0.06
Hα	0.03	−0.16
Hβ1	−0.13	−0.22
Hβ2	−0.16	−0.21
Hγ	−0.22	−0.22
Hδ	−0.39	−0.39
NCH_3	−0.96	−0.44
Gly	0.03	−0.06

[a]Conditions: 25°C, 10 mM Na_2DPO_4/NaD_2PO_4, pD 8.4 (uncorrected).

Binding Studies. Binding of $\mathbf{A}_2\mathbf{D}$ to histone 3 peptides containing Arg methylation at position 8[11] or KMe_3 at position 9[12] was determined to evaluate the selectivity for the different PTMs within the same sequence (Chart 1).[13] To determine the influence of the peptide sequence on recognition of $aRMe_2$, two additional biologically relevant Arg methylation sites were investigated, including histone 3 R2[14] and RUNX1 R210 (also known as AML1)[15] (Chart 1). Isothermal titration calorimetry (ITC) was performed to measure binding affinities (Table 2). The peptides were synthesized containing YGG at the N- or C-terminus for concentration determination by UV. We have

Chart 1. Peptide Sequences Used for ITC Binding Measurements Containing R, RMe, $aRMe_2$, $sRMe_2$, or KMe_3 as well as a YGG Sequence at the N- or C-Terminus for Concentration Determination

H3 R8Me_X (X = 0-2):	Ac-YGG-QTA(RMe_X)KSTG-NH_2
H3 K9Me_3:	Ac-YGG-QTAR(KMe_3)STG-NH_2
H3 R2Me_2:	A(RMe_2)TKQTA-GGY-NH_2
RUNX1 R210Me_2:	Ac-YGG-TAM(RMe_2)VSP-NH_2

Table 2. Dissociation Constants (K_d) and $\Delta G_{binding}$ for $\mathbf{A}_2\mathbf{D}$ Binding to the Peptides Shown in Chart 1 As Measured by ITC[a]

entry	peptide	charge	K_{d1} (μM)	ΔG_1 (kcal/mol)
1	H3 aR8Me_2	+2	5.1 ± 0.6	−7.2 ± 0.1
2	H3 sR8Me_2	+2	38.4 ± 4.8	−6.0 ± 0.1
3	H3 R8Me[b,c]	+2	26.0 ± 3.0	−6.3 ± 0.1
4	H3 K9Me_3[c]	+2	3.9 ± 0.5	−7.4 ± 0.1
5	H3R8K9[b,c]	+2	≥60	≤−5.7
6	H3 aR2Me_2[c]	+3	0.93 ± 0.01	−8.2 ± 0.1
7	H3 sR2Me_2	+3	2.3 ± 1.7	−7.7 ± 0.1
8	RUNX1 aR210Me_2	+1	6.4 ± 0.9	−7.1 ± 0.1
9	RUNX1 sR210Me_2	+1	18.1 ± 0.8	−6.5 ± 0.1

[a]Average of three runs, except where noted (see Supporting Information). Data fit to a two-site binding model. Error is from the standard deviation. Conditions: 25 °C, 10 mM Na_2HPO_4/NaH_2PO_4, pH 8.4. [b]Data fit to a one-site binding model. [c]Average of two runs.

dx.doi.org/10.1021/ja307907p | J. Am. Chem. Soc. 2013, 135, 6450−6455

shown that Tyr in the context of an unmodified peptide does not bind to **A_2D**, although we cannot exclude the possibility that the Tyr tag in the peptides used for ITC contributes to binding.[16] With the exception of H3 R8K9 and H3 R8Me, the ITC data were best fit with a model for two independent sites, giving two binding affinities representing a tight binding event and a weaker binding event that we expect is due to nonspecific interactions (see Supporting Information).[17]

The original receptor, **A_2B**, exhibits a binding affinity for H3 K9Me_3 of approximately 25 μM,[5] as measured by fluorescence anisotropy, with binding affinities >600 μM for all of the methylation states of H3 R8 (see Supporting Information). In contrast, **A_2D** exhibits a binding affinity of 5 μM for H3 aR8Me_2, with greater than 7-fold selectivity over H3 sR8Me_2 and more than 10-fold selectivity over the unmodified H3 peptide, H3 R8K9. The selectivity over H3 R8Me is slightly less, at about 5-fold, suggesting that the smaller RMe side chain can be accommodated better than the bulky sRMe_2. These results are qualitatively consistent with the amplifications observed in the DCLs (Figure 4b) and indicate that **A_2D** exhibits similar selectivity to many methyl Arg binding proteins (Table 3).

Table 3. Binding Affinities of Different Reader Proteins to Methyl Arg Containing Peptides

reader protein	methylation mark	K_d (μM)	ref
eTud11	Aub sR11Me_2	71	2a
eTud11	Aub sR13Me_2	48	2a
eTud11	Aub sR15Me_2	5.4	2a
SMN Tudor	sRMe_2[a]	476	2b
SMN Tudor	aRMe_2[a]	1025	2b
SPF30 Tudor	sRMe_2[a]	652	2b
SPF30 Tudor	aRMe_2[a]	1006	2b
SND1 eTudor	PIWIL1 sR4Me_2	10	2c
SND1 eTudor	PIWIL1 aR4Me_2	42	2c
SND1 eTudor	PIWIL1 R4Me	19	2c
SND1 eTudor	PIWIL1 R4	97	2c
TDRD1 TD2	sR45Me_2	55	3a
TDRD1 TD2	sRMe_2[a]	172	3a
TDRD1 TD3	sR74Me_2	35	3a
TDRD1 TD3	sRMe_2[a]	353	3a
TDRD3	PIWIL sRMe_2	>300	3b
TDRD3	PIWIL aRMe_2	>150	3b

[a]Reported K_d is for the amino acid alone.

Surprisingly, the binding affinity of **A_2D** for H3 K9Me_3 was found to be equivalent to that of H3 aR8Me_2, showing no distinction between the two modifications. It is worth noting that the similar affinity of **A_2D** for aRMe_2 and KMe_3 is not apparent from the **A_2D** amplification data alone. This can be explained by the fact that KMe_3 amplifies both **A_2D** and **A_3**, which compete for monomer **A** in the DCL. Thus, the extent of **A_2D** amplification by KMe_3 is lower than in the presence of aRMe_2, which does not significantly amplify either **A_3** receptor. This highlights the possible breakdown of the correlation between amplification and binding efficiency as a result of complex competing equilibria that minimize the overall free energy of the system.[9]

The binding affinities of **A_2D** to aRMe_2 and sRMe_2 were compared across all three peptides in Chart 1 to gain insight into the influence of the surrounding sequence on binding. While **A_2D** binds aRMe_2 more strongly than sRMe_2 in every case, the degree of selectivity appears to be somewhat influenced by the surrounding sequence, ranging from about 2.5- to 7.5-fold. This is likely due to variation in additional contacts made between the receptor and the peptide. The data in Table 2 suggest a modest influence of the sequence on binding based on net charge of the peptide, but the trend is not strong (compare entries 1, 6, and 8 and 2, 7, and 9). The peptides with a +3 charge bind more tightly than the others, but the peptides with a +1 and +2 charge are not significantly different. Thus, it may be that the location of the charge also influences binding affinity, through its ability to make a direct contact with the carboxylates on the exterior of the receptor. For example, if the H3 aR8Me_2 peptide adopts an extended conformation, K9 would be directed away from aR8Me_2, which may reduce its influence on binding, in contrast to K4 in the H3 aR2Me_2 peptide, which would be directed toward the receptor.

DISCUSSION AND CONCLUSIONS

Combined, these data provide insight into the binding affinity and selectivity of **A_2D** for methylated Arg. The selectivity for the different methylation states of Arg can be explained by differences in size, surface area, and desolvation costs. Binding of unmethylated Arg in aqueous solution has been reported with several synthetic receptors.[8,18] However, cation$-\pi$ interactions alone are typically not strong enough to result in binding due to the high desolvation cost of binding Arg in an aromatic pocket; generally, electrostatic interactions are also needed to achieve binding in aqueous solution.[8] Thus, as the carboxylates in monomer **A** are held outside of the binding pocket and the carboxylate in monomer **D** is in the same plane as the naphthalene, which is not optimal for binding Arg,[8,19] weak binding of unmethylated Arg by **A_2D** was expected.

Methylation of Arg reduces its desolvation cost by both reducing the number of hydrogen-bond donors on the guanidinium group and preventing the formation of bifurcated hydrogen bonds with water.[20] Additionally, increased methylation of Arg has been shown in other systems to make stacking interactions with aromatic rings more favorable.[21] Thus, binding of methylated arginines in an aromatic pocket of the appropriate size is expected to be able to overcome the desolvation cost.[8] Binding of aRMe_2 by **A_2D** is about 0.5 − 1.2 kcal/mol more favorable than binding of sRMe_2, depending on the peptide sequence. The magnitude of a cation$-\pi$ interaction is equivalent for the two isomers of RMe_2, and so that cannot account for the selectivity of **A_2D** for aRMe_2.[21] It may be that sRMe_2 is too large to effectively fit into the binding pocket, such that sRMe_2 can only insert one methylimminium group into the pocket. This is consistent with the NMR data, which exhibits half as much shifting of the methyl groups in sRMe_2 as observed for aRMe_2 as well as broadening of the methyl groups in sRMe_2. This would result in one less methyl$-\pi$ interaction than aRMe_2 and potentially place an N−H in the pocket instead, resulting in a higher desolvation penalty than for aRMe_2. The binding of RMe to **A_2D** is also weaker than the binding of aRMe_2. RMe can make fewer van der Waals contacts than aRMe_2, and it also has a higher desolvation cost, which can account for the 0.9 kcal/mol difference in binding affinities.

Interesting conclusions can also be drawn from a comparison of **A_2D** and **A_2B**. While **A_2B** exhibits a 2 kcal/mol difference in binding affinity for K9Me_3 relative to aR8Me_2, replacement of the phenyl ring in **A_2B** with the naphthyl ring in **A_2D** abolishes this selectivity. This gain in binding energy for aRMe_2 by **A_2D**

dx.doi.org/10.1021/ja307907p | J. Am. Chem. Soc. 2013, 135, 6450−6455

can be attributed to both the formation of a larger binding pocket, which can accommodate aRMe$_2$ and additional $\pi-\pi$ stacking interactions between aRMe$_2$ and the naphthyl ring.

The carboxylic acids in **A$_2$B** and **A$_2$D** do not appear to play a direct role in binding to the methylated side chain. It is well established that the carboxylates on monomer **A** are held rigidly outside of the cavity and do not contribute directly to binding of ammonium or guanidinium cations.[8] Additionally, the carboxylates on the aromatic rings of **B** and **D** are not oriented properly to interact directly with the cation in the binding pocket, as has been shown in other synthetic receptors for Lys and Arg.[8,19] Thus, it appears that a combination of cation$-\pi$ and van der Waals interactions is the primary driving force for binding both methylated side chains.[22] However, charged residues in the surrounding peptide appear to contribute additional electrostatic interactions with the carboxylates in a sequence-dependent manner. Modification of the carboxylates to create a neutral water-soluble receptor would likely abrogate any sequence selectivity and is currently under investigation.

The structures of protein binding pockets that recognize RMe$_2$ are all quite similar, consisting of a cube in which four faces consist of aromatic residues, the fifth face is a hydrogen-bonding group (typically Asn), and the sixth face is open to allow for entry of the RMe$_2$ side chain into the pocket (Figure 2).[2] **A$_2$D** loosely mimics this binding format, as it provides an aromatic pocket with five aromatic rings, although it lacks the hydrogen-bonding group directed into the pocket. Nonetheless, **A$_2$D** is still able to bind aRMe$_2$ more tightly than several of the RMe$_2$ binding proteins (see Table 3). This suggests that the aromatic cages in the native RMe$_2$ binding proteins are not necessarily optimal for binding of RMe$_2$ but rather provide the necessary degree of binding to result in the desired phenotype. Additionally, a comparison of **A$_2$D** to the binding pockets of RMe$_2$ binding proteins suggests that the introduction of a hydrogen bonding group in the appropriate location may further increase binding affinity and selectivity. This is an ongoing effort in our group.

In conclusion, we have identified a novel small molecule receptor, **A$_2$D**, for the recognition of aRMe$_2$. With the exception of antibodies,[23] to the best of our knowledge this is the only known synthetic receptor that recognizes aRMe$_2$ with selectivity over sRMe$_2$. **A$_2$D** exhibits comparable affinities and selectivites for the different methylation states of Arg as native methyl Arg binding domains. The low micromolar affinity of aRMe$_2$ by **A$_2$D** is impressive, as the primary driving force for binding is the interaction with the modified side chain, unlike many of the native proteins which recognize the surrounding residues and protein backbone as well. The preference for aRMe$_2$ over the other methylation states can be attributed to differences in the van der Waals contacts, cation$-\pi$ interactions, and desolvation penalties. The results presented here demonstrate the ability to develop and fine tune a receptor by making subtle changes to the building blocks used in DCC and suggest opportunities to further optimize function. Receptors of this type are promising for applications involving differential sensing of PTMs, such as pattern recognition assays or affinity chromatography.[24,25]

EXPERIMENTAL PROCEDURES

Synthesis of Monomer D. Synthesis of monomer **D** was achieved following a modified procedure for the synthesis of an isomeric compound, as described in the Supporting Information.[26]

Dynamic Combinatorial Chemistry. The relevant building blocks were individually dissolved in water, adding sufficient 1.0 M aqueous NaOH to fully deprotonate the thiols and carboxylic acids on the building blocks, using sonication when necessary. The pH of each solution was then adjusted to 8.5 using 1.0 M aqueous HCl and 1.0 M aqueous NaOH. Aliquots of each monomer solution were combined in a 2 mL LC-MS vial to reach a final concentration of 5 mM **A** and 2.5 mM **D**, respectively. When necessary, an aliquot of the appropriate peptide guest dissolved in water was added to the reaction to reach a final concentration of 7.5 mM peptide. Any remaining volume was made up with water. The vials were capped and analyzed by HPLC-MS at various time points.

Analytical LC-MS. LC-MS was carried out on an Agilent Rapid Resolution LC-MSD system equipped with an online degasser, binary pump, autosampler, heated column compartment, and diode array detector. All separations were performed using 5 mM NH_4OAc H_2O-acetonitrile gradients at pH 5 and a Halo C18 column (4.6 × 100 mm, 2.7 μm). The MS was performed using a single quad mass spectrometer. Mass spectra (ESI-) were acquired in ultrascan mode by using a drying temperature of 350 °C, a nebulizer pressure of 45 psi, a drying gas flow of 10 L/min, and a capillary voltage of 3000 V. The reactions were monitored weekly (3 μL injections) until equilibrium was reached after about 3 weeks.

Synthesis of A$_2$D. Biased libraries were prepared on a 0.05 mmol scale (**A**: 35.6 mg, 0.1 mmol, 6.67 mM; **D**: 11.8 mg, 0.05 mmol, 3.33 mM) templated with methylisoquinoline iodide (41.0 mg, 0.15 mmol, 10 mM). Methylisoquinoline iodide was used as the template as it is less expensive than the aRMe$_2$ peptide and also templates **A$_2$D** formation. Upon equilibration the libraries were neutralized, and the receptors were isolated by semipreparative HPLC. Approximately 0.3 mL injections were chromatographed using buffered mobile phases A (10 mM NH_4OAc in water) and B (10 mM NH_4OAc in 9:1 ACN to water) using a gradient (0−35% B from 0 to 5 min, then 35−70% B from 5 to 20 min) with a flow rate of 4.0 mL/min. A sharper **A$_2$D** peak was achieved with a column heater set to 40 °C, but this was not necessary for separation from the library. The **A$_2$D** peak at 13.5 min was collected and analyzed for purity by analytical LC-MS, giving a 45% yield (see Supporting Information). Purified **A$_2$D** was lyophilized to powder and stored under nitrogen.

NMR Characterization of A2D. All 1D and 2D NMR samples were prepared and analyzed on a Varian Inova 600 MHz instrument similar to those described previously, unless noted otherwise. For characterization, a 600 μM **A$_2$D** sample was prepared in 50 mM borate buffer at pD 9.25 containing 0.05 mM DSS. The 1D spectrum of **A$_2$D** was collected at 5 °C using 32 K data points and 900 scans with a 3 s presaturation. 2D NMR experiments used for structural analysis included COSY, TOSCY, and NOESY experiments. ^{1}H NMR (600 MHz, D_2O, borate buffer, pD 9.25, uncorrected): δ = 8.20 (s, 1H), 8.18 (s, 1H), 8.07 (s, 1H), 8.04 (d, 1H), 7.99 (s, 1H), 7.97 (d, 1H), 7.81 (d, 1H), 7.73 (s, 1H), 7.61 (d, 1H), 7.05 (d, 1H), 6.82 (s, 1H), 6.46 (d, 1H), 5.95 (s, 1H), 5.75 (d, 1H), 5.72 (s, 1H), 5.58 (s, 1H), 5.34 (d, 1H), 5.30 (s, 1H), 5.22 (s, 1H), 3.10 (dd, 1H), 2.93 (d, 1H).

NMR Analysis of Binding Interactions. NMR experiments were performed on 600 MHz Bruker NMR at 25 °C, in 10 mM Na_2DPO_4/NaD_2PO_4 (pD 8.0 = pH 8.4) buffer with DSS (2.0 mM) as an internal standard. Peptide stock solutions were made (20−24 mM), and concentration determined with respect to DSS by NMR. Peptides were diluted to a concentration of 600 μM. An NMR of each pure peptide was obtained for comparison, and the 600 μM peptide stock solution was then used to dissolve **A$_2$D** (3.2−3.5 equiv) to give a final concentration of 2−2.2 mM **A$_2$D** in 600 μM peptide. 1D spectra were collected for each sample with 128−512 scans. All Arg protons were assigned using TOCSY analysis with and without **A$_2$D** present.

Isothermal Titration Calorimetry. ITC titrations were performed on a Microcal AutoITC200. Titrations were carried out at 298 K in buffered H_2O (10 mM Na_2HPO_4/NaH_2PO_4, pH 8.4). The concentration of **A$_2$D** was determined by measuring the UV−vis absorbance at 267 nm, using a NanoDrop2000 with a xenon flash lamp, 2048 element linear silicon CCD array detector, and 1 mm path length. A 1−3 mM solution of peptide was titrated into an 80−200

μM solution of $\mathbf{A_2D}$, using 2.0 μL increments every 3 min. Heats of dilution were subtracted prior to fitting. Binding curves were produced using the supplied Origin software and fit using one- or two-site binding models.

■ ASSOCIATED CONTENT

Ⓢ Supporting Information

Synthesis, NMR characterization, and binding data. This material is available free of charge via the Internet at http://pubs.acs.org.

■ AUTHOR INFORMATION

Corresponding Author

mlwaters@unc.edu

Author Contributions

¶These authors contributed equally.

Notes

The authors declare no competing financial interest.

‡This author previously published under the name Lindsey A. Ingerman.

■ ACKNOWLEDGMENTS

We thank the Defense Threat Reduction Agency (DTRA) for support (HDTRA1-10-1-0030 and W911NF-06-1-0169). We also gratefully acknowledge support from the W. M. Keck Foundation. This material is based in part upon work supported by the National Science Foundation Graduate Research Fellowship to J.E.B. under grant no. DGE-1144081.

■ REFERENCES

(1) (a) Bedford, M. T.; Clarke, S. G. *Mol. Cell* **2009**, *33*, 1−13. (b) Bedford, M. T.; Richard, S. *Mol. Cell* **2005**, *18*, 263−272. (c) Di Lorenzo, A.; Bedford, M. T. *FEBS Lett.* **2011**, *585*, 2024−31.

(2) (a) Liu, H.; Wang, J.-Y.; Huang, Y.; Li, Z.; Gong, W.; Lehmann, R.; Xu, R.-M. *Genes Dev.* **2010**, *24*, 1876−81. (b) Tripsianes, K.; Madl, T.; Machyna, M.; Fessas, D.; Englbrecht, C.; Fischer, U.; Neugebauer, K. M.; Sattler, M. *Nat. Struct. Mol. Biol.* **2011**, *18*, 1414−21. (c) Liu, K.; Chen, C.; Guo, Y.; Lamb, R.; Bian, C.; Xu, C.; MacKenzie, F.; Pawson, T.; Min. *J. Proc. Natl. Acad. U.S.A.* **2010**, *107*, 18398−403.

(3) (a) Mathioudakis, N.; Palencia, A.; Kadlec, J.; Round, A.; Tripsianes, K.; Sattler, M.; Pillai, R. S.; Cusack, S. *RNA* **2012**, *18*, 2056−72. (b) Liu, K.; Guo, Y.; Liu, H.; Bian, C.; Lam, R.; Liu, Y.; Mackenzie, F.; Rojas, L. A.; Reinberg, D.; Bedford, M. T.; Xu, R.-M.; Min, J. *PLoS One* **2012**, *7*, e30375. (c) Sikorsky, T.; Hobor, F.; Krizanova, E.; Pasulka, J.; Kubicek, K.; Stefl, R. *Nucleic Acids Res.* **2012**, *40*, 11748−55.

(4) For reviews, see: (a) Corbett, P. T.; Leclaire, J.; Vial, L.; West, K. R.; Wietor, J.-L.; Sanders, J. K. M.; Otto, S. *Chem. Rev.* **2006**, *106*, 3652−3711. (b) Lehn, J.-M. *Chem.—Eur. J.* **1999**, *5*, 2455−2463. (c) Ladame, S. *Org. Biomol. Chem.* **2008**, *6*, 219−226. (d) Ludlow, R. F.; Otto, S. *Chem. Soc. Rev.* **2008**, *37*, 101−108. (e) Otto, S. *Curr. Opin. Drug Disc. Devel.* **2003**, *6*, 509−520.

(5) Ingerman, L. A.; Cuellar, M. E.; Waters, M. L. *Chem. Commun.* **2010**, *46*, 1839−41.

(6) (a) Otto, S.; Furlan, R. L. E.; Sanders, J. K. M. *J. Am. Chem. Soc.* **2000**, *122*, 12063−12064. (b) Ramström, O.; Lehn, J.-M. *ChemBioChem* **2000**, *1*, 41−48.

(7) (a) Hughes, R. M.; Waters, M. L. *J. Am. Chem. Soc.* **2005**, *127*, 6518−9. (b) Hughes, R. M.; Benshoff, M. L.; Waters, M. L. *Chem.—Eur. J.* **2007**, 5753−5764.

(8) Ngola, S. M.; Kearney, P. C.; Mecozzi, S.; Russell, K.; Dougherty, D. A. *J. Am. Chem. Soc.* **1999**, *121*, 1192−1201.

(9) Corbett, P. T.; Sanders, J. K. M.; Otto, S. *Chem.—Eur. J.* **2008**, *14*, 2153−2166.

(10) Concentration dependent NMR studies with $\mathbf{A_2D}$ revealed no signs of self-association.

(11) Blythe, S. A.; Cha, S.-W.; Tadjuidje, E.; Heasman, J.; Klein, P. S. *Dev. Cell* **2010**, *19*, 220−31.

(12) Kouzarides, T. *Cell* **2007**, *128*, 693−705.

(13) Binding affinities of $\mathbf{A_2B}$ to the different methylation states of Arg were measured by fluorescence anisotropy, as they had not been reported previously, confirming that $\mathbf{A_2B}$ binds all methylation states of Arg very weakly. See Supporting Information.

(14) (a) Guccione, E.; Bassi, C.; Casadio, F.; Martinato, F.; Cesaroni, M.; Schuchlautz, H.; Lüscher, B.; Amati, B. *Nature* **2007**, *449*, 933−937. (b) Hyllus, D.; Stein, C.; Schnabel, K.; Schiltz, E.; Imhof, A.; Dou, Y.; Hsieh, J.; Bauer, U. M. *Genes Dev.* **2007**, *21*, 3369−3380. (c) Iberg, A. N.; Espejo, A.; Cheng, D.; Kim, D.; Michaud-Levesque, J.; Richard, S.; Bedford, M. T. *J. Biol. Chem.* **2008**, *283*, 3006−3010.

(15) Zhao, X.; Jankovic, V.; Gural, Z.; Huang, G.; Pardanani, A.; Menendez, S.; Zhang, J.; Dunne, R.; Xiao, A.; Erdjument-Bromage, H.; Allis, C. D.; Tempst, P.; Nimer, S. D. *Genes Dev.* **2008**, *22*, 640−53.

(16) A control peptide containing Tyr but no methylated Lys or Arg was unable to displace a dye from $\mathbf{A_2D}$ in an indicator displacement assay, suggesting that Tyr alone does not bind. Peacor and Waters, unpublished results.

(17) Use of a two-site binding model increases the error in the enthalpy values. Thus, we have not attempted to interpret ΔH and ΔS from this binding data.

(18) (a) Bell, T. W.; Khasanov, A. B.; Drew, M. G. B.; Filikov, A.; James, T. *Angew. Chem., Int. Ed.* **1999**, *38*, 2543−2547. (b) Douteau-Gue vel, N.; Perret, F.; Coleman, A.; Morel, J.-P; Morel-Desrosiers, N. *J. Chem. Soc., Perkin Trans. 2* **2002**, 524−532. (c) Arnaud-Neu, F.; Fuangswasdi, S.; Notti, A.; Pappalardo, S.; Parisi, M. F. *Angew. Chem.* **1998**, *110*, 120−122; *Angew. Chem., Int. Ed.* **1998**, *37*, 112−114. (d) Fokkens, M.; Schrader, T.; Klärner, F.-G. *J. Am. Chem. Soc.* **2005**, *127*, 14415−14421.

(19) Rensing, S.; Arendt, M.; Springer, M.; Grawe, T.; Schrader, T. *J. Org. Chem.* **2001**, *66*, 5814−21.

(20) McQuinn, K.; McIndoe, J. S.; Hof, F. *Chem.—Eur. J.* **2008**, *14*, 6483−9.

(21) Hughes, R. M.; Waters, M. L. *J. Am. Chem. Soc.* **2006**, *128*, 12735−12742.

(22) Ma, J. C.; Dougherty, D. A. *Chem. Rev.* **1997**, *97*, 1303−1324.

(23) Boisvert, F.-M.; Cote, J.; Boulanger, M.-C.; Richard, S. Mol. *Cell. Proteomics* **2003**, *2*, 1319.

(24) Wiskur, S. L.; Ait-Haddou, H.; Lavigne, J. J.; Anslyn, E. V. *Acc. Chem. Res.* **2001**, *34*, 963−972.

(25) For a recent example, see: Minaker, S. A.; Daze, K. D.; Ma, M. C. F.; Hof, F. *J. Am. Chem. Soc.* **2012**, *134*, 11674−11680.

(26) West, K. R.; Ludlow, R. F.; Corbett, P. T.; Besenius, P.; Mansfeld, F. M.; Cormack, P. A. G.; Sherrington, D. C.; Goodman, J. M.; Stuart, M. C. A.; Otto, S. *J. Am. Chem. Soc.* **2008**, *130*, 10834−10835.